Quantum statistics in a time-modulated exciton-photon system

G. Yu. Kryuchkyan,[1,2,3] A. R. Shahinyan,[1,3] and I. A. Shelykh[4,5,6]

[1]*Center of Quantum Technologies and New Materials, Yerevan State University, Alex Manoogian 1, 0025 Yerevan, Armenia*

[2]*Armenian State Pedagogical University after Kh. Abovyan, Tigran Mets avenue 17, 0010 Yerevan, Armenia*

[3]*Institute for Physical Researches, National Academy of Sciences, Ashtarak-2, 0203 Ashtarak, Armenia*

[4]*Science Institute, University of Iceland, Dunhagi-3, IS-107 Reykjavik, Iceland*

[5]*Division of Physics and Applied Physics, Nanyang Technological University, Singapore 637371*

[6]*ITMO University, St. Petersburg 197101, Russia*

(Received 23 September 2015; revised manuscript received 1 December 2015; published 29 April 2016)

We consider a system consisting of a large individual quantum dot with excitonic resonance coupled to a single-mode photonic cavity in the nonlinear regime when exciton-exciton interaction becomes important. Quantum statistics of coupled exciton-photon modes is studied for two regimes of driving: a monochromatic input field and a field with periodically time-modulated amplitude. We show that sub-Poissonian statistics for both modes are realized in the case of monochromatic driving for transient and steady-state regimes in the presence of decoherence and cavity-induced feedback. We also demonstrate that variances of quantum fluctuations of photon and exciton numbers display oscillations in the case of modulated input. In this case, we show an improvement of the degree of sub-Poissonian statistics and antibunching for both modes at periodic sequence of definite time intervals in comparison with the case of the steady-state regime for monochromatic driving. We also observe the Wigner functions with negative values in phase space for a time-modulated exciton-photon system.

DOI: 10.1103/PhysRevA.93.043857

I. INTRODUCTION

Light-matter interaction usually is considered in two qualitatively different regimes, namely, weak and strong coupling. For the first of them the spectrum of the material system remains unchanged, and light-matter interaction results in single acts of the emission and absorption of the photons. On the contrary, in the regime of strong coupling light and matter can no longer be treated independently of each other, and hybrid half-light, half-matter modes appear in the system. Those modes are known as polaritons. Nowadays, the variety of polaritonic systems is impressive and includes such widely studied cases as surface plasmon polaritons [1] and cavity polaritons [2]. In the latter case the photonic mode is coupled with excitonic transition in the quantum well, quantum wire, or individual quantum dot (QD).

Coupling between the QD and photonic mode of a zero-dimensional cavity lies at the heart of a rapidly developing branch of science known as cavity quantum electrodynamics (cQED). The problem is important not only because of the fundamental aspects brought forward by the interaction of material systems with photons [3] but also because of the potential application of cQED to quantum information processing [4–6]. From the point of view of experimental realization, excitons in individual QDs can be brought to strong coupling with a confined electromagnetic mode provided by a pillar (etched planar cavity) [7], the defect of a photonic crystal [8], or the whispering gallery mode of a microdisk [9,10], among other things. In the regime of weak excitation such structures have demonstrated the Rabi doublet in their optical spectra, which is characteristic of the mode anticrossing that marks the overcoming of dissipation by the coherent exciton-photon interaction.

These achievements open the way to a new research area, namely, investigation of the pure quantum effects originating from strong exciton-photon coupling [11]. Although the system exhibits strong coupling, it is usually not known in which quantum state it is actually realized. For the system to be useful for quantum information applications, one should be able to manipulate not just the mean number of the particles in the system but also have a tool to monitor and control their statistics. In this context, the possibility to create states different from essentially classical coherent and thermal states is highly desirable. If the energy of the system scales linearly with the number of particles, it is essentially classical [12], and adding or removing a single particle will not change its behavior. Therefore, an analysis of the nonlinear effects is highly desirable.

With QDs in microcavities, two types of strong nonlinearities are expected, both associated with the excitons [13]. The first one comes from Pauli exclusion, which arises from the fermionic character of the particles forming an exciton. It becomes extremely important for the case of small QDs for which, similar to individual atoms, the excitation of more than one exciton becomes impossible. Pauli blocking leads to the radical transformation of the spectrum of the system, which changes from the Rabi doublet to the Mollow triplet when the intensity of the external pump is increased [14–18].

The second is Coulomb repulsion between the excitons, again arising from their composite nature. This mechanism is important for the case of the excitons in the quantum wells and large QDs. In the former case it leads to the blueshift of the polaritonic modes increasing with the intensity of the external pump, an effect which can be satisfactorily described within the framework of the mean-field approximation. The case of an individual large QD inside the cavity is, however, more tricky. Coulomb repulsion between the excitons in this configuration leads to the emergence of a rich multiplet structure in the emission spectrum [19], which reveals the pure quantum nature of light-matter coupling.

In the present paper we analyze further the quantum effects arising from nonlinearities in a coupled QD-cavity system for two cases of the external driving field: a cw monochromatic

field and a field with amplitude time-periodic modulations. The importance of the last regime stems from the idea that quantum effects can be modified if the system is driven by an external pump with fast time-periodic modulations. Particularly, it has been demonstrated that the application of a time-modulated cw field as well as a sequence of tailored pulses leads to an improvement of the degree of quantum effects in open-cavity nonlinear systems and the onset of qualitatively new quantum effects in the time domain. Indeed, it has been demonstrated that amplitude modulation can improve single-photon statistics in photon sources based on a quantum dot [20] and leads to the formation of a high degree of continuous-variable entanglement and squeezing in optical parametric oscillators [21–23] for definite time intervals. This approach was also recently exploited for generation of Fock states and effective multiphoton blockades in a Kerr nonlinear resonator driven by a sequence of Gaussian pulses [24–27]. The idea to enrich quantum physical systems by designing a time modulation has been explored in several other fields of research, including periodically driven nonlinear oscillator [28] and periodically driven quantum matter [29].

Here we focus on the consideration of cavity modes in regimes of strong exciton-photon coupling and strong exciton-exciton interaction with respect to the rates of damping of the photonic and excitonic modes. In these regimes the transition frequencies between the energy levels of the systems without any interaction with the external field are spectacularly distinguishable in the quantum regime. Thus, we enable spectroscopic identification and selective excitation of transitions between combined exciton-number–photon-number states.

This consideration is done in the framework of the master equation and the numerical calculation of quantum trajectories and is based on the calculations of excitation numbers, the Q Mandel parameter, the second-order correlation functions, and the Wigner functions of exciton and photonic modes that allow phase-space monitoring of exciton-photon coupling in the quantum treatment.

In regimes of strong coupling we observe a quantum effect of sub-Poissonian statistics of both photon and exciton modes via the monochromatic driving field for all time intervals, including the transient regime and the steady-state regime for time intervals exceeding the characteristic time of dissipative processes, $t \gg \gamma^{-1}$. In the regime of time modulation the ensemble-averaged mean photon numbers, the populations of photon-number and exciton-number states, and the Wigner functions are nonstationary and exhibit a periodic time-dependent behavior, i.e., repeat the periodicity of the pump laser for time intervals over transient dynamics. We also demonstrate that the application of a time-modulated field leads to improving the degree of sub-Poissonian statistics of modes for definite time intervals in comparison with the analogous results for the case of monochromatic excitation. In addition to this we observe that the Wigner functions with negative values in the phase space showing quantum interference are realized due to time modulation. The results can be directly applied in time-resolved quantum technologies. In addition to this we investigate temperature noisy effects for a cavity at finite temperatures. This leads to applications in simulating more realistic exciton-photon systems as well as to the study of unusual quantum phenomena connecting quantum engineering and temperature.

This paper is organized as follows. In Sec. II we present the effective Hamiltonian for the periodically driven polariton system and describe the physical quantities of interest. In Sec. III we study quantum statistics and the Wigner functions of exciton and photon modes in the steady-state regime as well as for the case of time-modulated external pumping. We analyze also the distributions of photon-number states and the phase-space properties of photon and exciton-modes on the basis of the Wigner functions. The effects of a thermal reservoir are also briefly analyzed. We summarize our results in Sec. IV.

II. COUPLED EXCITON-PHOTON SYSTEM

The system consists of coupled fundamental photonic dot and exciton modes driven by a cw field with mean frequency ω and time-modulated amplitude. The Hamiltonian of the driven photon-exciton system in the rotating-wave approximation (RWA) reads

$$H = \Delta_{ph} a^\dagger a + \Delta_{ex} b^\dagger b + \chi {b^\dagger}^2 b^2 + g(b a^\dagger + b^\dagger a) + [\Omega_1 + \Omega_2 \exp(-i\delta t)]a + \text{H.c.}, \tag{1}$$

where $a^\dagger$ and a are creation and annihilation operators of the photon mode, $b^\dagger$ and b are creation and annihilation operators for the exciton mode, g is the exciton-photon coupling constant, χ is the strength of the exciton-exciton interaction, and $\Delta_{ph} = \omega_{ph} - \omega$ and $\Delta_{ex} = \omega_{ex} - \omega$ are detunings between the mean frequency of the driving field and the frequencies of the photonic and exciton modes. Ω_1 and Ω_2 are the components of the complex amplitude of the driven field, and δ is the frequency of the modulation. Such a situation can also be realized if the photon-exciton system is driven by two fields with different frequencies. In this case, the Hamiltonian of the system in the RWA is reduced to Eq. (1), with δ being the difference between frequencies of the driving fields. The case $\Omega_2 = 0$ describes the exciton-photon cavity driven by a cw monochromatic field treated within the RWA.

In realistic systems one should necessarily take into account the dissipation because the modes suffer from losses due to partial transmission of light through the mirrors of the photonic cavity, nonradiative decay of excitons, and decoherence. We consider these effects by assuming that the interaction of the driven photon-exciton system with a heat reservoir gives rise to the damping rates of modes γ_a and γ_b. We trace out the reservoir degrees of freedom in the Born-Markov limit assuming that the system and environment are uncorrelated at initial time $t = 0$. This procedure leads to the master equation for the reduced density matrix in the Lindblad form. The master equation within the framework of the rotating-wave approximation in the interaction picture corresponding to the transformation $\rho \to e^{-i\omega a^+ at} \rho e^{i\omega a^+ at}$ reads

$$\frac{d\rho}{dt} = -i[H,\rho] + \sum_{i=1,2,3,4} \left(L_i \rho L_i^\dagger - \frac{1}{2} L_i^\dagger L_i \rho - \frac{1}{2} \rho L_i^\dagger L_i \right), \tag{2}$$

where $L_1 = \sqrt{(n_{th}+1)\gamma}\, a$, $L_2 = \sqrt{n_{th}\gamma}\, a^+$, $L_3 = \sqrt{(n_{th}+1)\gamma}\, b$, and $L_4 = \sqrt{n_{th}\gamma}\, b^+$ are the Lindblad

operators, γ is a dissipation rate, and n_{th} denotes the mean number of quanta of a heat bath. Here for simplicity we assume that the decay rates and the mean numbers of quanta of a heat bath are equal for both modes, $\gamma_a = \gamma_b = \gamma$.

We analyze the mean values of excitation numbers, and we also probe the strength of quantum fluctuations of exciton and photonic modes via the Mandel factor and the normally ordered second-order correlation functions of the photon numbers and excitation numbers. In addition we monitor the phase properties of both modes using the Wigner function. The quantities of interest are calculated by using the reduced density operators of the photons $\rho_a(t)$ and of the excitons $\rho_b(t)$. These operators are constructed from the full-density operator of the system $\rho(t)$ by tracing out the excitonic and photonic modes, respectively,

$$\rho_a(t) = \mathrm{Tr}_b(\rho), \tag{3}$$

$$\rho_b(t) = \mathrm{Tr}_a(\rho). \tag{4}$$

For the system under time-modulated external pumping the ensemble-averaged excitation numbers of the modes as well as the other physical quantities exhibit a periodic time-dependent behavior after transient time intervals. Using the master equation, we calculate the time evolution of the Q Mandel factor for the photonic and exciton modes. For the photonic mode it is defined as

$$Q(t) = \frac{\langle [\Delta n(t)]^2 \rangle - \langle n(t) \rangle}{\langle n(t) \rangle}, \tag{5}$$

where $\langle [\Delta n(t)]^2 \rangle = \langle (a^\dagger a)^2 \rangle - (\langle a^\dagger a \rangle)^2$ describes the deviation of the excitation number uncertainty from the Poissonian variance, $\langle (\Delta n)^2 \rangle = \langle n \rangle$. The case $Q = 0$ corresponds to Poissonian statistics. If $Q > 0$, the statistics is super-Poissonian; if $Q < 0$. it is sub-Poissonian, and the statistics is analogous for the exciton mode.

The Mandel factor is connected to the normalized second-order correlation function for zero delay time $g^{(2)}$, defined (for the photonic mode) as

$$g^{(2)}(t) = \frac{\langle a^\dagger(t) a^\dagger(t) a(t) a(t) \rangle}{[\langle a^\dagger(t) a(t) \rangle]^2}. \tag{6}$$

For short counting time intervals the approximate relation between these quantities reads $\langle (\Delta n)^2 \rangle = \langle n \rangle + \langle n \rangle^2 (g^{(2)} - 1)$. Thus, the condition $g^{(2)} < 1$ corresponds to the sub-Poissonian statistics, $\langle (\Delta n)^2 \rangle < \langle n \rangle$.

We analyze the master equation numerically using the well-known quantum state diffusion method [30]. According to this method, the reduced density operator is calculated as the ensemble mean over the stochastic states describing evolution along a quantum trajectory.

It should be mentioned that the exciton-photon system can actually be presented as the model of coupled photonic resonators with anharmonic terms when only one of the cavity modes is driven resonantly. In this case the exciton-photon coupling constant corresponds to the tunnel coupling rate between two resonators. Such a model has been the focus of considerable attention, and this interest is justified by many applications in different contexts. Particularly, in the field of quantum devices on a few-photon level one application concerns the realization of the so-called unconventional photon blockade originating from the destructive interference between different paths from the ground state to two-photon states in two coupled photonic cavities with Kerr nonlinearities that are very small compared to the mode decay rates [31–35]. In the regime of optimal one-photon blockade weak Kerr nonlinearity is required only for the auxiliary cavity that is not laser driven, and hence, the coupled-resonators model is described by the Hamiltonian (1). This mechanism of an unconventional photon blockade is valid for weak pumping conditions, leading to very small mean excitation numbers of the cavity mode. In this paper we consider the other regime of a strong Kerr nonlinearity for the exciton mode, leading to quantum effects for comparatively large excitation numbers of both photonic and excitonic modes.

III. SUB-POISSONIAN STATISTICS, ANTIBUNCHING, AND WIGNER FUNCTIONS FOR COUPLED EXCITON-PHOTON MODES

In our further consideration we concentrate on the analysis of coupled exciton-photon modes in quantum regimes at a low level of quanta. This analysis is performed by using the set of dimensionless parameters Δ/γ, χ/γ, g/γ, as well as parameters of amplitude modulation Ω_1/γ, Ω_2/γ and the frequency of modulation δ.

Let us discuss the operational regimes in more detail. If the energy levels of the coupled exciton-photon states are well resolved, we can consider selective transitions near resonance between lower photon-exciton states. In this way, the detunings play an important role when identifying the spectral lines; thus, we arrange the detunings of modes to reach a qualitative quantum effect. We estimate the detuning by using the results on the structure of energy levels of a quantum dot in a microcavity in the nonlinear regimes [19]. In this paper the optical spectrum at the resonance transition was studied by diagonalizing the Hamiltonian (1) without the driving term. In this case the total number of excitations is conserved, and eigenstates of the total particle number $a^\dagger a + b^\dagger b$ with the eigenvalue m can be used as the mth manifold of the system. Particularly, two-photon excitation of the system with $m = 2$ leads to eigenvectors that involve triplet states $|2,0\rangle$, $|1,1\rangle$, $|0,2\rangle$ with photon- and exciton-number states. If we neglect the exciton-exciton interaction, the energy levels form the Rabi triplet $E_+ = 2\omega_{ph} + 2g$, $E_0 = 2\omega_{ph}$, $E_- = 2\omega_{ph} - 2g$. In this way, the two-photon resonant frequency leading to excitation of the level E_- equals $2\omega_2 = E_- - E_g$, where E_g is the level of the ground state. Therefore, $\omega_2 = \omega_{ph} - g$, and hence, the detunings $\Delta_{ex} = \omega_{ex} - \omega_2$, $\Delta_{ph} = \omega_{ph} - \omega_2$ are $\Delta_{ph} = \Delta_{ex} = g$. In this approach the effects of exciton-exciton interaction can be included by using the numerical calculations [19]. For the strong driving field the detunings can also be shifted due to Stark effects. Thus, for the concrete calculations, later we use the approximate value of detunings corresponding to the parameters g/γ and χ/γ. Note that such analysis seems to be qualitative rather than quantitative but allows us to estimate the values of detunings.

Indeed, considering the analysis of the selective excitation of cavity modes, we need to consider the other resonant frequencies corresponding to large numbers of quanta, $m > 2$.

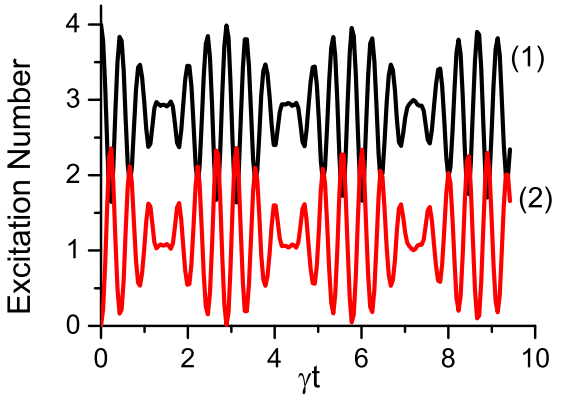

FIG. 1. Time evolution of the mean excitation numbers of photonic (1) and excitonic (2) modes for the nondissipative case, without any driving. The parameters are as follows: $\Delta_{ph}/\gamma = \Delta_{ex}/\gamma = 7.12$, $g/\gamma = 5$, $\chi/\gamma = 4$.

Below, for the concrete calculations we use the values $\Delta_{ph}/\gamma = \Delta_{ex}/\gamma = 7.12$ that are estimated for the parameter $g/\gamma = 7$.

For illustrative purposes let us first consider the case of the nondissipative system. The typical results for the time evolution of the mean excitation numbers of both the photon mode and the exciton mode due to the coupling between modes and the exciton-exciton nonlinearity are shown in Fig. 1. We assume that at $t = 0$ the exciton mode is in vacuum state $\langle n(0)\rangle_b = 0$ while the four-photon number state is injected into the resonator, $\langle n(0)\rangle_a = 4$. As we see, without any driving, the total number of quanta is conserved, and the dynamics of the excitation numbers displays oscillatory behavior, where the Rabi transitions between the modes with collapses and revival effects are observed.

The collapses and revivals are well-known phenomena in quantum optics, particularly in the context of the Jaynes-Cummings model (see, for example, [36]) and for ion-trap systems [37,38]. Here we obtain interesting collapses and revival effects in the simplest model as a manifestation of nonlinear exciton-exciton interaction that leads to spaced energies of exciton-number states. Also note that in this case conservation of total particle numbers leads to antiphase dynamics of the mode that is violated in the presence of driving.

A. Quantum statistics in the case of monochromatic driving

Now, we turn to the realistic case in which dissipation and decoherence are taken into account considering pure quantum effects for a zero-temperature cavity. We start from the case of $\Omega_2 = 0$, which corresponds to the single monochromatic excitation and the initial state corresponding to no excitations in the cavity. The typical results for the excitation numbers, the Mandel parameters, and the contour plots of the Wigner functions of two modes are depicted in Fig. 2. As we see, the mean excitation numbers and the Mandel parameter show Rabi-type oscillations for short time intervals in the transient regime and reach equilibrium in the steady-state regime. From Fig. 2(a) we conclude that for the parameters used the system is operated in a strong quantum regime at the level of small excitation numbers. In the steady-state regime, the exciton

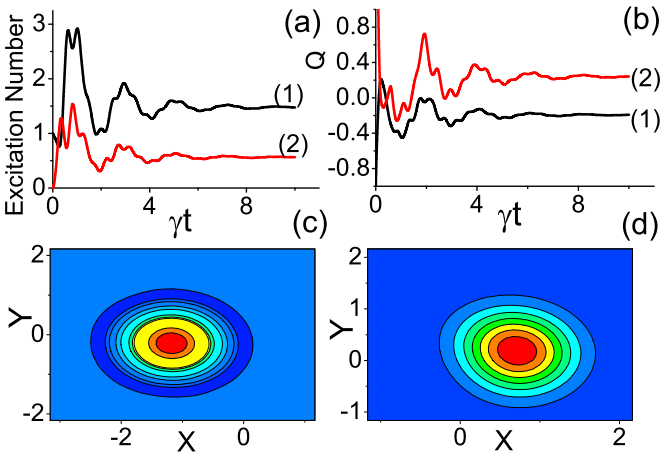

FIG. 2. The results for the case of single-mode driving, $\Omega_2 = 0$. (a) Temporal dependence of the mean excitation numbers of photonic (1) and excitonic (2) modes; (b) temporal dependence of the Mandel parameters for photonic (1) and excitonic (2) modes. The contour plots of the Wigner functions of (c) the photonic mode and (d) excitonic mode for time intervals corresponding to the maximal values of excitation numbers. The parameters are as follows: $\Delta_{ph}/\gamma = 7.12$, $\Delta_{ex}/\gamma = 7.12$, $g/\gamma = 5$, $\chi/\gamma = 1$, $\Omega_1/\gamma = 5$, $\Omega_2/\gamma = 0$.

Mandel parameter $Q_b > 0$, while $Q_a = -0.2$; that is, the photonic mode displays sub-Poissonian statistics. The Wigner functions of both modes are positive in the entire phase space, but contours of the Wigner function for the photonic mode have a slightly squeezed form corresponding to small sub-Poissonian statistics.

Below we discuss how the statistics of the modes, particularly the bunching of the exciton mode and the antibunching of the photon mode in the monochromatic excitation regime, are changed by increasing the amplitude of the driving field. In Fig. 3 we show the excitation numbers and the Mandel parameters for a comparatively large value of the amplitude, $\Omega_1/\gamma = 10$. It can be seen that, naturally, the level of mean excitation numbers increases as a function of amplitude. We also observe that in this regime both modes, photonic and excitonic, display sub-Poissonian statistics and antibunching. Increasing the external field amplitude leads to a decrease in the Mandel parameter [in Fig. 3(b) $Q_a = -0.6$, while $Q_a = -0.2$ in Fig. 2(b)].

In Fig. 3(d) we demonstrate that increasing the coupling constant of the exciton-photon coupling and the strength of exciton-exciton nonlinear interaction makes quantum effects more pronounced. Increasing these parameters leads to increasing the mean excitation number of the photonic mode and to decreasing the Mandel factors. Naturally, the question of which parameter is exactly responsible for that arises. The analysis shows that both processes stipulated by the parameters χ/γ and g/γ are responsible for such behavior. To clarify this point we turn to the analogous effects for a single driven anharmonic oscillator with Kerr nonlinearity. In this system, the efficiency of the quantum effects requires a high nonlinearity χ with respect to dissipation, and increasing the parameter χ/γ leads to a decrease of the mean excitation number of the oscillatory mode (see, for example, [25]). As we

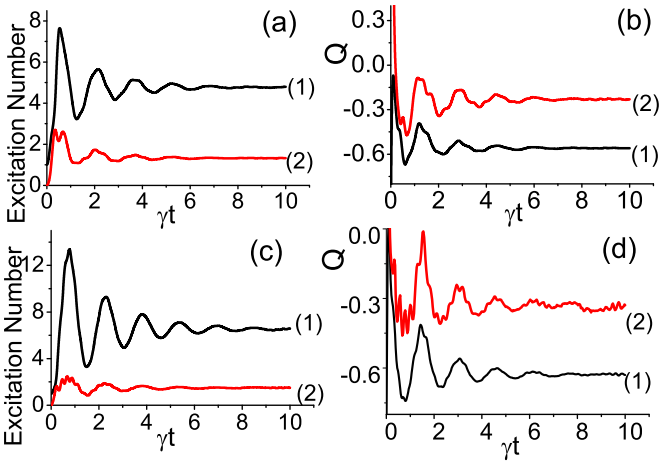

FIG. 3. The results for the case of single-mode driving, $\Omega_2 = 0$, where curves (1) correspond to the photonic mode and curves (2) correspond to the excitonic mode. (a) and (c) Temporal dependence of the mean excitation numbers of modes; (b) and (d) temporal dependence of the Mandel parameters for excitonic and photonic modes. The parameters are as follows: $\Delta_{ph}/\gamma = 7.12$, $\Delta_{ex}/\gamma = 7.12$, $g/\gamma = 5$, $\chi/\gamma = 1$, $\Omega_1/\gamma = 10$, $\Omega_2/\gamma = 0$, $\delta/\gamma = 0$ in (a) and (b); $\Delta_{ph}/\gamma = 7.12$, $\Delta_{ex}/\gamma = 7.12$, $g/\gamma = 7$, $\chi/\gamma = 3$, $\Omega_1/\gamma = 10$, $\Omega_2/\gamma = 0$ in (c) and (d).

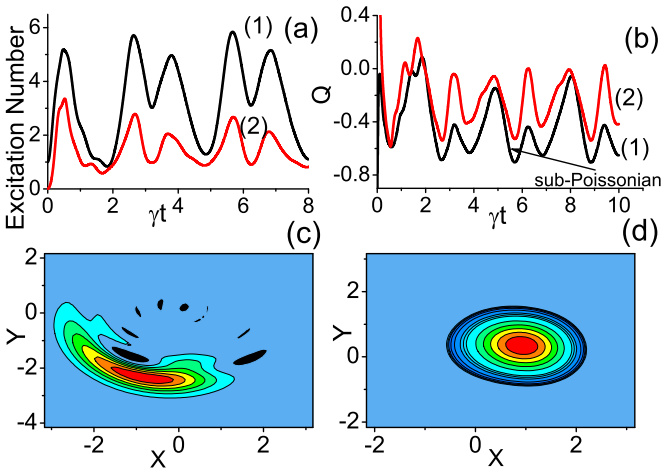

FIG. 4. The results for the case of a periodically driven photon-exciton system. Curves (1) correspond to the photonic mode, and curves (2) correspond to the excitonic mode. (a) Temporal dependence of the mean excitation numbers for both modes, (b) temporal dependence of the Mandel parameters for both modes, (c) the Wigner function of the photonic mode corresponding to the maximal occupancy of the mode, and (d) the Wigner function of the photonic mode corresponding to the minimal occupancy of the mode. The parameters are as follows: $\Delta_{ph}/\gamma = 7.12$, $\Delta_{ex}/\gamma = 7.12$, $g/\gamma = 5$, $\chi/\gamma = 1$, $\Omega_1/\gamma = 5$, $\Omega_2/\gamma = 5$, $\delta/\gamma = 2$.

see, the situation is different from the analogous one for two coupled oscillators realized for the exciton-photon system.

As the numerical calculations show for the exciton-photon system, the mean excitation number of the excitonic mode decreases with the increase of the nonlinearity parameter, while the mean excitation number of the photonic mode increases with the nonlinearity parameter. For the coupling constant g/γ we have different behavior; increasing the coupling parameter increases the levels of excitation numbers of both modes.

B. Quantum statistics in the case of time-modulated driving

The typical results for the case of time-modulated driving with $\Omega_2 \neq 0$ are presented in Figs. 4, 5, 6, and 8 for various parameters of the exciton-photon system. As one can see in Figs. 4(a) and 4(b), for the parameters $\chi/\gamma = 1$ and $g/\gamma = 5$, the mean excitation numbers and the Mandel parameters repeat the periodicity of the input field in an over-transient regime. It is remarkable that time modulation of modes leads to the formation of highly sub-Poissonian statistics compared with the case of monochromatic driving [see the results depicted in Figs. 2(a), 2(b), 3(a), and 3(b)]. Indeed, in the case of time modulation the values of the Mandel parameter can reach the values of $Q_a \approx -0.65$ for the photonic mode and $Q_b \approx -0.45$ for the exciton mode at definite time intervals. To be correct we compare the results for two-field pumping [Figs. 4(a) and 4(b)] with the results for one-mode pumping in the cw regime [Figs. 3(a) and 3(b)] at the same total pumping intensity. Thus, if one compares these values of Mandel parameters with those obtained earlier for single-mode cw pumping, one can make the conclusion that quantum effects in the exciton-photon system become more pronounced for the case of time-modulated pumping for a periodic sequence of definite time intervals. We also note that the maximal degree of sub-Poissonian statistics is realized for the time intervals corresponding to the maximal values of the occupations of the modes. Thus, the quantum effects are most essential for a comparatively large number of quanta.

The contour plots of the Wigner functions for maximal and minimum values of the photonic mode are presented in Figs. 4(c) and 4(d), respectively. We observe that the Wigner function corresponding to the maximal values of the photon excitation number displays negative values in the phase – space (these regions are shown in black), which means quantum interference is realized in this regime. For time intervals corresponding to the minimal photon numbers the Wigner

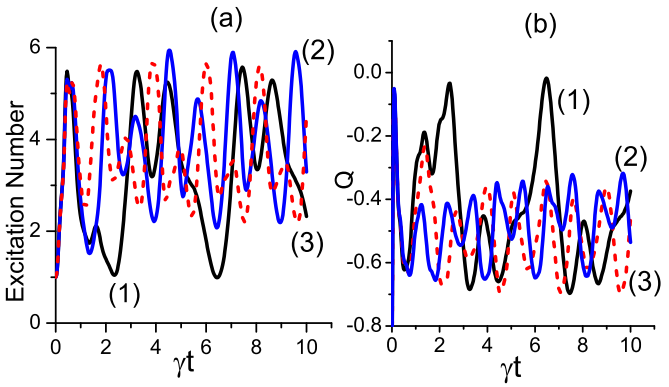

FIG. 5. (a) The mean excitation number and (b) Q factor depending on time intervals for various values of the modulation frequency: $\delta/\gamma = 1.5$, curve (1), $\delta/\gamma = 2.5$, curve (2), $\delta/\gamma = 3$, curve (3). The parameters are as follows: $\Delta_{ph}/\gamma = 7.12$, $\Delta_{ex}/\gamma = 7.12$, $g/\gamma = 5$, $\chi/\gamma = 1$, $\Omega_1/\gamma = 5$, $\Omega_2/\gamma = 5$.

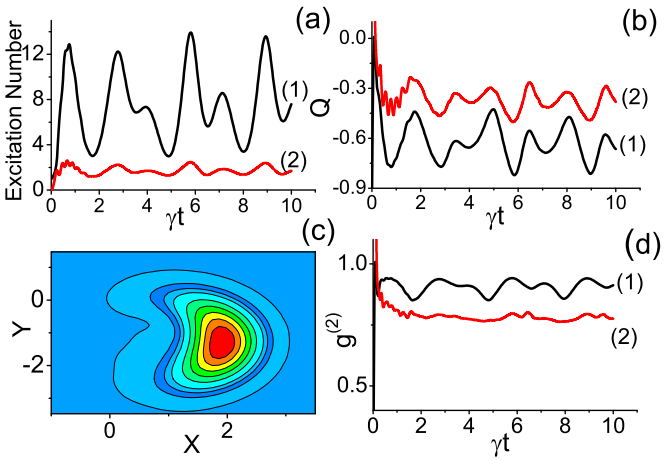

FIG. 6. The results for the case of the periodically driven photon-exciton system in the deeply sub-Poissonian regime. Curves (1) correspond to the photonic mode, and curves (2) correspond to the excitonic mode. (a) Time dependence of the mean excitation numbers, (b) time dependence of the Mandel parameters, (c) the contour plots of the Wigner function corresponding to the maximal occupancy of the photonic mode, and (d) time-dependent normalized second-order correlation functions for photonic and exciton modes. The parameters are as follows: $\Delta_{ph}/\gamma = 7.12$, $\Delta_{ex}/\gamma = 7.12$, $\chi/\gamma = 3$, $g/\gamma = 7$, $\Omega_1/\gamma = 5$, $\Omega_2/\gamma = 5$, $\delta/\gamma = 2$.

function for the photonic mode is positive in the entire phase space and have a slightly squeezed form corresponding to sub-Poissonian statistics.

As the numerical analysis shows, the improvement of sub-Poissonian statistics occurs for a period of modulation comparable to the characteristic time of dissipation γ^{-1} and disappears for asymptotic cases of slow frequency $\delta/\gamma < 1$ and fast frequency $\delta/\gamma > 1$ modulations. This situation for three different values of the ratio, $\delta/\gamma = 1.5$, $\delta/\gamma = 2.5$, and $\delta/\gamma = 3$, is shown in Fig. 5. Comparing time-dependent Mandel parameters for different ratios δ/γ with the analogous results depicted in Fig. 4(b), we can see that a more efficient effect of sub-Poissonian statistics takes place for the optimal value $\delta_{op}/\gamma = 2$ used in Fig. 4(b). As the calculations show, variations of the modulation frequency from its optimal value lead to a decrease of the Q factor and the degree of the sub-Poissonian statistics. It is interesting to compare the optimal modulation frequency with the frequency of damped Rabi-type oscillations δ_R that take place for the main excitation numbers and Q factor at short time intervals for the case of the monochromatic excitation. From the data of Figs. 3(a) and 3(b) we estimate the Rabi frequency as $\delta_R/\gamma = 5.2$, which is noticeably larger than the value obtained for the optimal frequency. Thus, the effect of improving the degree of the sub-Poissonian statistics via modulation takes place for a time interval that exceeds the period of the Rabi-type oscillations.

It seems intuitively clear that such an achievement is due to the control of quantum dissipative dynamics as well as the quantum noise level through the application of a suitable tailored, time-dependent driving field. Indeed, the suppression of quantum fluctuations in time-modulated optical parametric oscillator and nondegenerate optical parametric oscillator [21,23] has been demonstrated in the frame of the analytical solution of the stochastic equations of motion. It was shown that this effect is stipulated by multiplicative noise terms for which the stochastic noise correlators also include the time-modulated amplitude of the input field. On the whole time modulation significantly improves the degree of squeezing and continuous-variable entanglement in the time domain.

We also note that the regime of time modulation is analogous (preferable for the case of $\Omega_1 = \Omega_2$) to excitation of the system by a sequence of identical pulses. In this field, generation of the nonclassical states of light for various systems has been analyzed for time-domain operations. The improvement of photon statistics by choosing the parameters (mainly amplitude, shape, and pulse duration) of the driving laser pulses has also been shown [20,22,25,39,40]. Thus, there is an analogy between the observed effects on modification of quantum statistics of the exciton-photon system by time modulation and the above-mentioned previous results for pulsed regimes.

Increasing the exciton-photon coupling constant and the strength of exciton-exciton nonlinear interaction makes quantum effects more pronounced, as shown in Fig. 6 for both excitonic and photonic modes and for the parameters $\chi/\gamma = 3$, $g/\gamma = 7$. Note that for these parameters the detunings $\Delta_{ph}/\gamma = 7.12$, $\Delta_{ex}/\gamma = 7.12$ approximately correspond to two-photon selective excitation of the level E_- from the vacuum state, as has been shown above. Time evolution of the mean excitation numbers is depicted in Fig. 6(a). Comparing these results with analogous ones shown in Fig. 4(a), we conclude that increasing the parameters χ/γ and g/γ while leaving the other parameters the same leads to increasing the level of photon excitation numbers and decreasing the excitation numbers of the exciton mode. Considering the quantum statistics of modes [see Fig. 6(b)], we conclude that this regime displays a deeply sub-Poissonian statistics with the Mandel parameter achieving values of $Q_a \approx -0.8$ for the photonic mode and $Q_b \approx -0.5$ for the excitonic mode in their minima. Comparing these results with the results for the monochromatic pumping regime [Fig. 3(d)] with the same total pumping intensities, we can conclude that enhancement of these quantum effects is indeed due to time modulation of the exciton-photon system.

It is also interesting to present results for quantum statistics of the exciton-photon system within the framework of the normalized second-order correlation function by using the above formulas. The results for nonstationary correlation functions for photonic and excitonic modes versus dimensionless time intervals are depicted in Fig. 6(d). As we see, the correlation functions display antibunching for exciton and photon modes for all time intervals. However, the degree of antibunching for the exciton mode is slightly stronger than that for the photonic mode.

In addition, the correlation function of the exciton mode shows monotonous time behavior, with $g^{(2)} \approx 0.76$, while the analogous result for the photonic mode is nonmonotonous with $g^{(2)} \approx 0.82$ at its minimum value at definite time intervals corresponding to the minimal values of the mean photon number. For the comparison note that for the pure Fock state $|2\rangle$ the normalized second-order photon correlation function is equal to 0.5. Thus, the obtained results reflect excitations of states with high-order $m > 2$ manifolds and probably describe

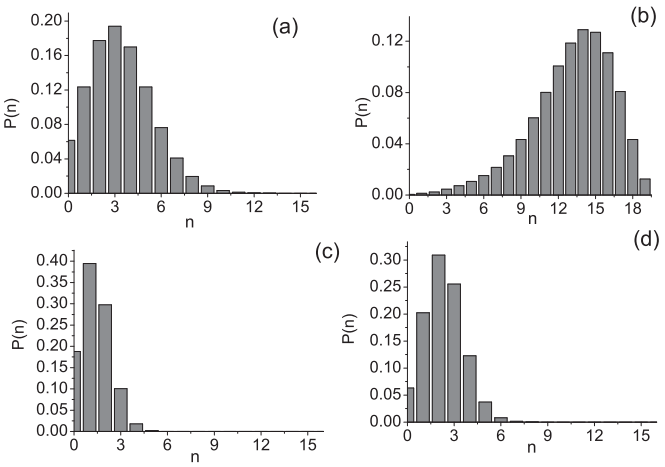

FIG. 7. The photon number distributions (a) at the minimum level of quanta and (b) at the maximum level of quanta. The exciton number distributions (c) at the minimum level of quanta and (d) at the maximum level of quanta. The parameters are as follows: $\Delta_{ph}/\gamma = 7.12$, $\Delta_{ex}/\gamma = 7.12$, $\chi/\gamma = 3$, $g/\gamma = 7$, $\Omega_1/\gamma = 5$, $\Omega_2/\gamma = 5$, $\delta/\gamma = 2$.

antibunching of photon-exciton states for a moderate number of quanta. A more complete description of the system can be obtained by calculating the Wigner function in phase space. In this way, the contour plots of the Wigner function for the photonic mode depicted in Fig. 6(c) display the typical form corresponding to light with sub-Poissonian statistics.

Additionally, the probability distributions of photon-number and exciton-number states for the definite time intervals are presented in Fig. 7. These results show that nonselective excitations of both photonic and excitonic modes are realized for the parameters used. Indeed, the distributions of photon numbers are relatively large and centered around the maximal and minimal values of the mean photon number [see Figs. 6(a) and 6(b)]. Nevertheless, the distributions considerably differ from the Poissonian distribution. The distributions of exciton numbers correspond to excitations of the mode at the level of a few quanta, in accordance with the results of mean exciton numbers.

It is interesting to analyze the minimal values of the Mandel factor in its time evolution for various exciton-photon coupling constants and strengths of exciton-exciton nonlinear interaction. The results for the photonic mode depending on the coupling constant g/γ are presented in Fig. 8 for three values of the parameter χ/γ and a fixed value of the amplitude of the driving field. One can clearly see that for the definite parameters of the driving time-dependent field, exciton-exciton interaction, and the detunings an optimal value of the ratio g/γ exists for which the quantum effects in the behavior of the system become the most pronounced. These results indicate the regime presented in Fig. 6 is the most preferable one for production of strong sub-Poissonian statistics.

C. Discussion of thermal effects

Now, we turn to the thermal effects, considering briefly the interaction of the exciton-photon system with the reservoir at finite temperatures. We investigate how the temperature

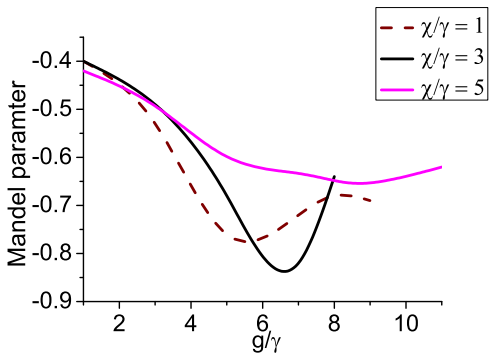

FIG. 8. The minimal values of the Mandel parameter depending on the exciton-photon coupling strength for several values of the exciton-exciton interaction: $\chi/\gamma = 1$, dashed curve; $\chi/\gamma = 3$, solid black curve; $\chi/\gamma = 5$, solid pink curve. The parameters are $\Delta_{ph}/\gamma = 7.12$, $\Delta_{ex}/\gamma = 7.12$, $\Omega_1/\gamma = 5$, $\Omega_2/\gamma = 5$, $\delta/\gamma = 2$.

affects the Mandel factor and the correlation function of the photon mode in comparison to the case of a zero-temperature reservoir. The effects of the thermal reservoirs are interesting for carrying out a more realistic approach to generating nonclassical states in exciton-photon systems and for studying phenomena connecting quantum engineering and temperature.

The results for the thermal photons in the range $n_{th} = 0.01 - 1$ are shown in Figs. 9(a) and 9(b). Taking into account that $T = \hbar\omega_{th}/k_B$, for the frequencies of thermal photons $\omega_{th} = 10$ GHz the temperature in this range corresponds to 10^{-1}–10 K. In order to illustrate the difference from the case of a zero-temperature resonator we assume here the same parameters as in the previous case depicted in Fig. 4. As our calculation shows, the maximal values of the mean photon numbers and the mean exciton numbers are approximately the same as in the case of a pure resonator, while the quantum statistics of the oscillatory modes is changed due to the thermal noise. The light inside the cavity remains sub-Poissonian and antibunched for all time intervals if $n_{th} = 0.05$. In this case the minimal values of the Q parameter and the correlation function remain close to the case of a vacuum reservoir. As expected,

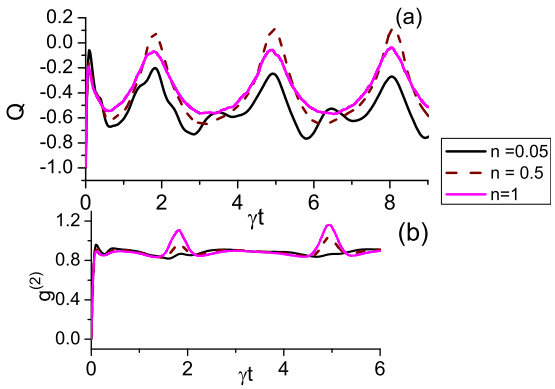

FIG. 9. (a) Time evolution of the Mandel factor for three values of thermal photon numbers n_{th}; (b) the second-order correlation function versus time intervals for several numbers of thermal photons. The parameters are as follows: $\Delta_{ph}/\gamma = 7.12$, $\Delta_{ex}/\gamma = 7.12$, $\chi/\gamma = 1$, $g/\gamma = 5$, $\Omega_1/\gamma = 5$, $\Omega_2/\gamma = 5$, $\delta/\gamma = 2$.

further increasing the temperature leads to a decrease of the quantum effects.

IV. CONCLUSION

In conclusion, we have considered the quantum statistics of a coupled exciton-photon system for two regimes of mode excitations: a cw monochromatic field and a time-modulated pump field. The temporal behavior of the mean excitation numbers of quanta, the Mandel parameter, the second-order correlation function, and the Wigner function of exciton and photon modes have been studied in the case of strong exciton-photon coupling and exciton-exciton interaction. We have demonstrated that results obtained by numerically solving the master equation have a strong dependence on the properties of the input driving. In this way, sub-Poissonian statistics for both modes has been observed in the case of monochromatic driving for all time intervals including transient and steady-state regimes. We have illustrated how the degree of sub-Poissonian statistics is controlled by exciton-photon and exciton-exciton couplings and the intensity of the pump field.

We have also investigated in detail nonlinear and quantum effects of the exciton-photon system driven by a time-modulated external field. Such amplitude modulation can be realized electronically using standard techniques, particularly with the help of an electro-optic amplitude modulator. Alternatively, amplitude modulation can be achieved in the system driven by a bichromatic pump field.

In the regime of time modulation the ensemble-averaged mean photon numbers, the populations of photon-number and exciton-number states, and the Wigner functions are nonstationary and exhibit a periodic time-dependent behavior, i.e., repeat the periodicity of the input for time intervals over transient dynamics. We have shown that the time-modulated exciton-photon system provides an effective mechanism for the improvement of the degree of sub-Poissonian statistics and antibunching for both modes in comparison with the monochromatic driving even in the presence of decoherence and cavity-induced feedback. The nonclassical states with strong sub-Poissonian statistics are formed for definite time intervals corresponding to the maximal values of the occupations of the modes depending on the modulation frequency, nonlinear coupling constants, the detunings, and driving input intensity. Thus, oscillations of both the variance of quantum fluctuations $\langle[\Delta n(t)]^2\rangle$ and the level of antibunching have been also observed. Further, a Wigner function with negative values in the phase space, showing quantum interference, has been observed for the time-modulated exciton-photon system.

We would like to underline that results for the time-modulated exciton-photon system have been obtained in time domain, without any time averaging, and hence can be directly applied in areas of time-resolved quantum measurements and quantum technologies (see, for example, [41,42]). In this field, the sources of nonclassical states must be operated in the pulsed or time-modulated regimes. In this way, the exciton-photon system interacting with a periodically modulated external field could be a good quantum device for producing high-degree sub-Poissonian and antibunched photons and excitons at periodic sequences of definite time intervals.

ACKNOWLEDGMENTS

We thank Prof. Yu. G. Rubo, Dr. A. Sheremet, and Prof. O. V. Kibis for the discussions we had on the subject. This work was supported by FP7 ITN "NOTEDEV", EC for the RISE Project CoExAN GA644076, and the Armenian State Committee of Science, Project No.15T-1C052. A.R.S. and G.Yu.K. thank the University of Iceland for hospitality.

[1] J. M. Pitarke, V. M. Silkin, E. V. Chulkov, and P. M. Echenique, Rep. Prog. Phys. **70**, 1 (2007).
[2] A. Kavokin, J. J. Baumberg, G. Malpuech, and F. P. Laussy, *Microcavities* (Oxford University Press, New York, 2007).
[3] H. Mabuchi and A. C. Doherty, Science **298**, 1372 (2002).
[4] A. Imamoglu, D. D. Awschalom, G. Burkard, D. P. Di Vincenzo, D. Loss, M. Sherwin, and A. Small, Phys. Rev. Lett. **83**, 4204 (1999).
[5] C. H. Bennett and D. P. DiVincenzo, Nature (London) **404**, 247 (2000).
[6] D. E. Chang, V. Vuletic, and M. D. Lukin, Nat. Photonics **8**, 685 (2014).
[7] J. P. Reithmaier, G. Sek, A. Löffler, C. Hofmann, S. Kuhn, S. Reitzenstein, L. V. Keldysh, V. D. Kulakovskii, T. L. Reinecker, and A. Forchel, Nature (London) **432**, 197 (2004).
[8] T. Yoshie, A. Scherer, J. Heindrickson, G. Khitrova, H. M. Gibbs, G. Rupper, C. Ell, O. B. Shchekin, and D. G. Deppe, Nature (London) **432**, 200 (2004).
[9] E. Peter, P. Senellart, D. Martrou, A. Lemaitre, J. Hours, J. M. Gerard, and J. Bloch, Phys. Rev. Lett. **95**, 067401 (2005).
[10] M. A. Kaliteevski, S. Brand, R. A. Abram, A. Kavokin, and L. S. Dang, Phys. Rev. B **75**, 233309 (2007).
[11] G. Khitrova, H. M. Gibbs, M. Kira, S. W. Koch, and A. Scherer, Nat. Phys. **2**, 81 (2006).
[12] Y. Zhu, D. J. Gauthier, S. E. Morin, Q. Wu, H. J. Carmichael, and T. W. Mossberg, Phys. Rev. Lett. **64**, 2499 (1990).
[13] F. P. Laussy, A. Kavokin, and G. Malpuech, Solid State Commun. **135**, 659 (2005).
[14] A. Muller, E. B. Flagg, P. Bianucci, X. Y. Wang, D. G. Deppe, W. Ma, J. Zhang, G. J. Salamo, M. Xiao, and C. K. Shih, Phys. Rev. Lett. **99**, 187402 (2007).
[15] E. B. Flagg, A. Muller, J. W. Robertson, S. Founta, D. G. Deppe, M. Xiao, W. Ma, G. J. Salamo, and C. K. Shih, Nat. Phys. **5**, 203 (2009).
[16] S. Ates, S. M. Ulrich, A. Ulhaq, S. Reitzenstein, A. Looffler, S. Hofling, A. Forchel, and P. Michler, Nat. Photonics **3**, 724 (2009).
[17] E. del Valle and F. P. Laussy, Phys. Rev. Lett. **105**, 233601 (2010).
[18] F. P. Laussy, E. del Valle, and C. Tejedor, Phys. Rev. Lett. **101**, 083601 (2008).
[19] E. del Valle, F. P. Laussy, F. M. Souza, and I. A. Shelykh, Phys. Rev. B **78**, 085304 (2008).

[20] A. Faraon, A. Majumdar, and J. Vuckovic, Phys. Rev. A **81**, 033838 (2010).
[21] H. H. Adamyan and G. Yu. Kryuchkyan, Phys. Rev. A **74**, 023810 (2006).
[22] N. H. Adamyan, H. H. Adamyan, and G. Yu. Kryuchkyan, Phys. Rev. A **77**, 023820 (2008).
[23] H. H. Adamyan, J. A. Bergou, N. T. Gevorgyan, and G. Yu. Kryuchkyan, Phys. Rev. A **92**, 053818 (2015).
[24] T. V. Gevorgyan, A. R. Shahinyan, and G. Yu. Kryuchkyan, Phys. Rev. A **79**, 053828 (2009).
[25] T. V. Gevorgyan, A. R. Shahinyan, and G. Yu. Kryuchkyan, Phys. Rev. A **85**, 053802 (2012).
[26] G. H. Hovsepyan, A. R. Shahinyan, and G. Yu. Kryuchkyan, Phys. Rev. A **90**, 013839 (2014).
[27] S. Ates, I. Agha, A. Gulinatti, I. Rech, A. Badolato, and K. Srinivasan, Sci. Rep. **3**, 1397 (2013).
[28] M. I. Dykman, in *Fluctuating Nonlinear Oscillators* (Oxford University Press, Oxford, 2012), pp. 167–194.
[29] N. Goldman, J. Dalibard, M. Aidelsburger, and N. R. Cooper, Phys. Rev. A **91**, 033632 (2015).
[30] N. Gisin and I. C. Percival, J. Phys. **25**, 5677 (1992); **26**, 2233 (1993); **26**, 2245 (1993); I. C. Percival, *Quantum State Diffusion* (Cambridge University Press, Cambridge, 2000).
[31] T. C. H. Liew and V. Savona, Phys. Rev. Lett. **104**, 183601 (2010).
[32] M. Bamba, A. Imamoglu, I. Carusotto, and C. Ciuti, Phys. Rev. A **83**, 021802(R) (2011).
[33] A. Majumdar, A. Rundquist, M. Bajcsy, and J. Vuckovic, Phys. Rev. B **86**, 045315 (2012).
[34] O. Kyriienko, I. A. Shelykh, and T. C. H. Liew, Phys. Rev. A **90**, 033807 (2014).
[35] H. Flayac, D. Gerace, and V. Savona, Sci. Rep. **5**, 11223 (2015).
[36] J. H. Eberly, N. B. Narozhny, and J. J. Sanchez-Mondragon, Phys. Rev. Lett. **44**, 1323 (1980); H. I. Yoo and J. H. Eberly, Phys. Rep. **118**, 239 (1985).
[37] For the experimental observation of Jaynes-Cummings revivals in Paul traps, see D. M. Meekhof, C. Monroe, B. E. King, W. M. Itano, and D. J. Wineland, Phys. Rev. Lett. **76**, 1796 (1996).
[38] M. Jakob and G. Yu. Kryuchkyan, Phys. Rev. A **59**, 2111 (1999).
[39] L. Qiu, L. Gan, W. Ding, and Z.-Y. Li, J. Opt. Soc. Am. B **30**, 1683 (2013).
[40] A. Rundquist, M. Bajcsy, A. Majumdar, T. Sarmiento, K. Fischer, K. G. Lagoudakis, S. Buckley, A. Y. Piggott, and J. Vuckovic, Phys. Rev. A **90**, 023846 (2014).
[41] S. Dambach, B. Kubala, V. Gramich, and J. Ankerhold, Phys. Rev. B **92**, 054508 (2015).
[42] B. Brecht, D. V. Reddy, C. Silberhorn, and M. G. Raymer, Phys. Rev. X **5**, 041017 (2015).